Unimolecular processes in CH_2OH below the dissociation barrier: O–H stretch overtone excitation and dissociation

Jie Wei, Boris Karpichev, and Hanna Reisler[a)]
Department of Chemistry, University of Southern California, Los Angeles, California 90089-0482

(Received 28 April 2006; accepted 26 May 2006; published online 17 July 2006)

The OH-stretch overtone spectroscopy and dynamics of the hydroxymethyl radical, CH_2OH, are reported in the region of the second and third overtones, which is above the thermochemical threshold to dissociation to $H+CH_2O$ ($D_0=9600\ cm^{-1}$). The second overtone spectrum at $10\,484\ cm^{-1}$ is obtained by double resonance IR-UV resonance enhanced multiphoton ionization (REMPI) spectroscopy via the $3p_z$ electronic state. It is rotationally resolved with a linewidth of $0.4\ cm^{-1}$ and displays properties of local-mode vibration. No dissociation products are observed. The third overtone spectra of CH_2OH and CD_2OH are observed at $\sim 13\,600\ cm^{-1}$ by monitoring H-atom photofragments while scanning the excitation laser frequency. No double resonance REMPI spectrum is detected, and no D fragments are produced. The spectra of both isotope analogs can be simulated with a linewidth of $1.3\ cm^{-1}$, indicating dissociation via tunneling. By treating the tunneling as one dimensional and using the calculated imaginary frequency, the barrier to dissociation is estimated at about $15\,200\ cm^{-1}$, in good agreement with theoretical estimations. The Birge-Sponer plot is linear for OH-stretch vibrations $1\nu_1-4\nu_1$, demonstrating behavior of a one-dimensional Morse oscillator. The anharmonicity parameter derived from the plot is similar to the values obtained for other small OH containing molecules. Isomerization to methoxy does not contribute to the predissociation signal and the mechanism appears to be direct O–H fission via tunneling. CH_2OH presents a unique example in which the reaction coordinate is excited directly and leads to predissociation via tunneling while preserving the local-mode character of the stretch vibration. © *2006 American Institute of Physics*. [DOI: 10.1063/1.2216703]

I. INTRODUCTION

The hydroxymethyl (CH_2OH) radical and its isomer, the methoxy (CH_3O) radical, have long been implicated in diverse areas such as atmospheric chemistry,[1] surface reactions,[2] and combustion chemistry.[3] Unimolecular processes in CH_3O and CH_2OH on the ground state potential energy surface (PES) have attracted considerable experimental and theoretical attention,[4–8] and it was found that both radicals have low dissociation barriers. *Ab initio* calculations show that the reaction barrier for the loss of hydrogen atom from CH_3O is lower than that for isomerization to CH_2OH.[6,7] In the case of CH_2OH, the situation is not as clear because the calculated barriers to direct O–H bond breaking and dissociation through isomerization are comparable, both leading to H atom and formaldehyde. According to calculations, the former is slightly higher than the latter.[6,7]

The quantum state resolved unimolecular dynamics for CH_3O in highly vibrationally excited states (up to $10\,000\ cm^{-1}$) have been examined by stimulated emission pumping (SEP) spectroscopy.[5,9–11] It was concluded that competition between intramolecular vibrational energy redistribution (IVR) and unimolecular decomposition was important in the vibrationally excited state, but there was no indication of isomerization. SEP experiments cannot be performed with CH_2OH, because its electronic excited states are dissociative with lifetimes shorter than 0.5 ps,[12–17] and so far no information on its unimolecular reaction on the ground state has been reported.

The photodissociation of CH_2OH radicals in excited electronic states has been examined experimentally[12–14,16,17] and theoretically.[15,18–20] The lowest excited electronic state, $3s$, internally converts to the ground state through efficient conical intersections that take place at long O–H distances, and the subsequent dissociation at low energies above the $3s$ onset gives rise exclusively to O–H bond breaking. When initial excitation accesses the $3p_x$ and $3p_z$ states, sequential couplings to the $3s$ state followed by conical intersections with the ground state propel the system to dissociation along the O–H and C–H dissociation coordinates. No isomerization to methoxy has been detected.[13,14,17]

The present study concerns the excitation and predissociation of CH_2OH on the ground PES by overtone OH-stretch excitation. Optical excitation of overtones has been used before to access highly vibrationally excited levels in the ground electronic state of stable molecules, e.g., HOOH, NH_2OH, and CH_3OH.[21–25] For example, in methanol OH-stretch (ν_1) overtones up to $5\nu_1$ have been excited directly,[21,22] and levels as high as $8\nu_1$ have been reached by using double resonance overtone excitation.[22] The IVR rates deduced for HOOH, NH_2OH, and CH_3OH were rather similar.[23]

There are two main differences between these studies and the one reported here. First and most important, in the

[a)]Author to whom correspondence should be addressed. Electronic mail: reisler@usc.edu

other studies the excited OH vibration was not the reaction coordinate and had a much higher bond energy than the lowest dissociation energy. Thus, high overtone excitation could be achieved in a potential that behaved as a local-mode Morse oscillator, and IVR preceded dissociation. In contrast, in CH_2OH the O–H bond is the reaction coordinate to H $+CH_2O$ and therefore it is not clear how high the OH-stretch vibration can be optically excited. Second, the species excited here is a free radical, adding the challenge of working with a minor component that is reactive.

Previously, we reported spectroscopic studies in the region of the CH and OH fundamental transitions and first overtone of the OH-stretch vibration in CH_2OH, and compared the experimental results to *ab initio* calculations.[26] Rotationally resolved spectra were recorded by double resonance ionization detection (DRID) via the $3p_z$ Rydberg state and showed line broadenings in the $2\nu_1$ spectrum that were thought to arise from low-order resonances. Here, we extend our studies to levels up to $4\nu_1$ ($13\,600\ cm^{-1}$), thereby approaching the dissociation barrier. By using DRID, we recorded a rotationally resolved spectrum of the second OH-stretch overtone. In contrast, the spectra obtained for CH_2OH and CD_2OH by exciting the $4\nu_1$ level could only be recorded by detecting hydrogen fragments and were partially rotationally resolved. We conclude that this state is predissociative and discuss linewidth broadening and predissociation via tunneling.

II. EXPERIMENT

The experimental methods for generating hydroxymethyl radicals in a molecular beam and their detection by time-of-flight (TOF) mass spectroscopy are described in detail elsewhere.[16] Reactant mixtures of Cl_2 (1%), CH_3OH (3%), and He are prepared in a glass bulb (5.0 l) at a total pressure of 2.0 atm at room temperature. The mixture is transported to the vacuum chamber through a piezoelectrically controlled pulsed nozzle.

Hydroxymethyl radicals are produced at the end of a quartz tube attachment to the nozzle aperture by the following reactions:

$$Cl_2 \xrightarrow{h\nu} 2Cl,$$

$$CH_3OH + Cl \rightarrow CH_2OH + HCl.$$

Photodissociation of Cl_2 is achieved with the 355 nm tripled output of a Nd:YAG (yttrium aluminum garnet) laser (Spectra Physics GCR-11, 6 mJ) focused by a 30 cm focal length (fl) cylindrical lens at the edge of the quartz tube. In order to minimize contributions from secondary reaction products,[13] CH_2OH radicals generated at the leading edge of the molecular beam pulse are probed. The molecular beam enters the detection chamber through a skimmer (Beam Dynamics, 1.50 mm). The rotational temperature of the radicals in the molecular beam is typically 10–15 K. The pressure in the detection region is $\sim 2.0\times 10^{-7}$ Torr with the nozzle operating at 10 Hz, and the base pressure is below 2.0×10^{-8} Torr. Spectra are obtained by exploiting pump and probe techniques, with different experimental schemes used for detection of $3\nu_1$ and $4\nu_1$ levels, as described below.

The experimental schemes for detection of $3\nu_1$ are similar to those used for the fundamental and the first overtone transitions, namely, depletion and DRID.[26] The main difference is that in this work we use (2+2) resonance enhanced multiphoton ionization (REMPI) with visible radiation to probe the radical,[8,16] instead of the (1+1) REMPI employed before.[26] The (2+2) scheme gives better signal-to-noise ratio (S/N), particularly in the DRID experiments. Detailed descriptions of the depletion and DRID schemes are given elsewhere.[26] Briefly, in depletion the pump wavelength is scanned with the probe wavelength fixed at a resonance for the (2+2) REMPI transition to $3p_z$. Because of the low depletion depth for overtone transitions and fluctuations in the (2+2) REMPI signal, this method gives lower S/N than DRID. In DRID, the pump wavelength is first fixed at the deepest depletion value, and the probe wavelength scanned in search of the 1_3^3 resonance for the CH_2OH (2+2) REMPI transition via $3p_z$, which has a favorable Franck-Condon factor. Once the transition is found, the probe is fixed at the resonance peak wavelength and the pump is scanned to obtain the second overtone transition spectrum. To distinguish between signal and background contributions, "pump-on" and "pump-off" experiments are carried out. The pump laser is fired 8 ns before the probe laser in a typical pump-on experiment, whereas the pump laser is set to fire ~ 1 μs later than the probe under pump-off conditions.

The pump radiation required for $3\nu_1$ excitation (around 954 nm) is obtained as the idler output of a seeded Nd:YAG laser pumped optical parametric oscillator (OPO) (Continuum, PL8000/Sunlite, 12 mJ; 0.1 cm^{-1}, 20 cm fl lens), and the probe radiation around 490 nm is generated by another Nd:YAG laser pumped dye laser (Continuum, ND6000, 0.1 cm^{-1}, 25 cm fl lens). In depletion experiments, a typical probe laser energy is 0.8 mJ, whereas in DRID experiments energies up to 4 mJ are used to increase the S/N.

With third overtone ($4\nu_1$) excitation, no depletion or DRID signal is observed above the background, but H-atom fragments are detected by (1+1′) REMPI via the $L\alpha$ hydrogen transition. Vacuum ultraviolet (vuv) radiation at 121.6 nm is obtained by frequency tripling 365 nm radiation (2 mJ) in a Kr/Ar filled cell, as described before.[13,14] The pump radiation is obtained from another Nd:YAG laser pumped dye laser (Continuum, ND6000, 35 mJ; 0.1 cm^{-1}, 25 cm fl lens). Action spectra in the $4\nu_1$ region are obtained by monitoring hydrogen fragments while varying the pump wavelength. In order to elucidate the role of isomerization, experiments were also carried out with CD_2OH (Aldrich, 99.5%-d) with the probe tuned, in turn, to detect H and D fragments.

In our experimental arrangement, the probe and pump laser beams are counterpropagating and cross the molecular beam at a right angle at the center of the repeller and accelerator plates of the vertically mounted TOF mass spectrometer. The ions are detected mass selectively. The output of a 25 mm diameter dual microchannel plate (MCP) detector (Galileo) is amplified with a wide-band preamplifier (KOA microcircuits, KE104), and the signal is digitized by a 500 MHz oscilloscope (Tektronix, TDS640A). The timing

sequence is controlled by two pulse generators (Stanford Research Systems). The lasers, pulse generators, and digitized oscilloscope are controlled with LABVIEW computer programs. Laser wavelengths are calibrated with a wavemeter (Burleigh WA-4500).

The TOF mass spectrometer is used in two modes. For mass resolution, the repeller and accelerator voltages are held at 3000 and 2330 V, respectively, to assure full separation of the masses of methanol and hydroxymethyl. For the TOF analysis required to obtain hydrogen translational energies, the repeller and extractor voltages are lowered to 360 and 280 V, respectively, while maintaining space-focusing conditions. At these voltages, the TOF traces have sufficient resolution to distinguish between hydrogen fragments generated by one- and two-photon dissociation. Unfortunately, at the lower voltages required to achieve full core-sampling conditions,[13,14] the S/N is too low, precluding a full analysis of the kinetic energy distributions.

III. RESULTS AND ANALYSIS

A. Excitation of the second OH-stretch overtone, $3\nu_1$

The second overtone of the OH-stretch of CH_2OH was observed by depletion and DRID in a similar manner to the fundamental and first overtone transitions.[26] In depletion spectroscopy, the pump laser was scanned while the probe laser was fixed to monitor the (2+2) REMPI signal of CH_2OH via the $3p_z \leftarrow 1A''$ 0_0^0 transition.[8,16] A maximum depletion signal ($\sim$10%) was recorded at 10 489.8 cm^{-1}. The narrow REMPI probe band obtained via the 0_0^0 transition makes depletion a convenient method. The S/N, however, is low because of the low intensity of the overtone transition and the fluctuations in the (2+2) REMPI signal and molecular beam intensity. Nevertheless, depletion gives an initial indication of the transition frequency to be used in the DRID experiments. In the DRID method, the probe transition originates in $3\nu_1$ and terminates in a vibrational state in $3p_z$ for which a favorable Frank-Condon factor exists.

In Fig. 1, the (2+2) REMPI signal of CH_2OH^+ is monitored by scanning the probe wavelength while keeping the pump frequency at 10 489.8 cm^{-1}, i.e., the $3\nu_1(^qR(2))$ frequency (see assignments below). Three "hot bands," 6_1^0, 8_2^0, and 9_2^0, are observed under both pump-on and pump-off conditions.[8] The peak signal of the origin band (41 068 cm^{-1}; not shown in Fig. 1) is two orders of magnitude higher in intensity than the hot bands.

The band appearing at 40 320±15 cm^{-1} only under pump-on conditions is assigned as 1_3^3. Previously, vibronic transitions originating in ν_1 and $2\nu_1$ in the ground electronic state were assigned as 1_1^1 and 1_2^2.[26] The propensity for the $\Delta v=0$ sequence for OH-stretch transitions to Rydberg states is explained by the nearly equal OH bond lengths in the CH_2OH neutral and cation.[8] For example, the DRID signal from the 1_1^1 band is three times more intense than the one from the 1_1^0 band. The energy of the $3\nu_1$ level in the $3p_z$ Rydberg state is determined at 9741±15 cm^{-1} above the origin by adding the pump laser frequency and the two-photon probe laser frequency and subtracting the 0_0^0 frequency. The assignment of the resonant level in $3p_z$ to $3\nu_1$ is confirmed by the Birge-Sponer relationship discussed below.

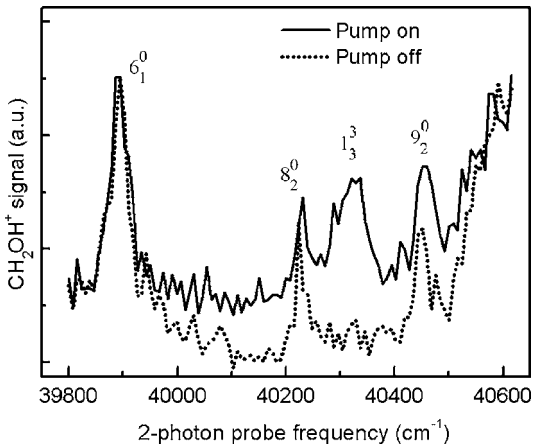

FIG. 1. IR+UV double resonance REMPI spectrum of CH_2OH obtained via the $3p_z$ state under "IR on" (solid line) and "IR off" (dotted line) conditions. The pump laser frequency is fixed at 10 489.8 cm^{-1}, the frequency of the second overtone transition in CH_2OH. The probe laser frequency is scanned and the (2+2) REMPI signal is recorded. The x axis denotes the probe frequency required to access the $3p_z$ state. In addition to several vibronic hot bands, which appear both under "pump-on" and "pump-off" conditions, the 1_3^3 band appears only when the pump laser is on.

By scanning the pump laser wavelength while keeping the probe at the two-photon peak transition, the rotationally resolved $3\nu_1$ DRID spectrum shown in Fig. 2(a) is obtained. This scheme takes advantage of the broad linewidth of the 1_3^3 transition (60 cm^{-1}, see Fig. 1). A simulated spectrum obtained by using the asymmetric rotor program ASYROTWIN (Ref. 27) is shown in Fig. 2(b) (see Sec. IV for details).

In order to get a rough estimate of the lifetime of CH_2OH in $3\nu_1$, the time delay between the pump and probe lasers was varied while monitoring the CH_2OH^+ DRID sig-

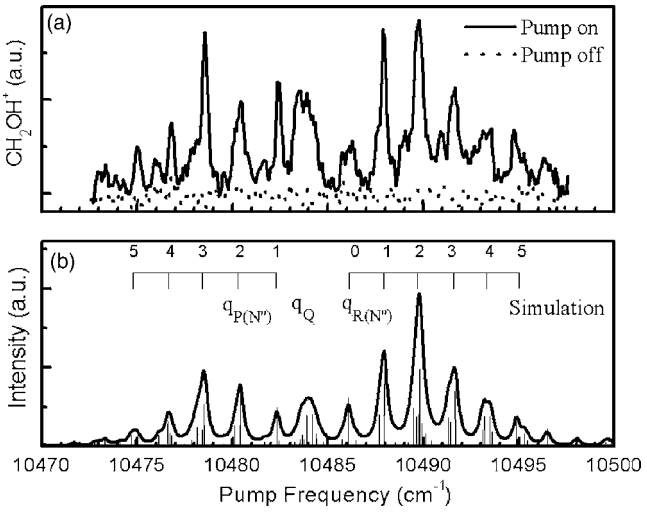

FIG. 2. IR spectrum of CH_2OH in the region of the second overtone of the OH stretch obtained by DRID. The upper panel displays the experimental spectrum. The solid and dotted lines represent signals corresponding to "IR-on" and "IR-off" experiments, respectively. In the bottom panel a best-fit spectrum with a linewidth of 0.4 cm^{-1} is shown. The calculated rotational transitions are given by the stick spectrum. In the simulations, we used A'' =6.51 cm^{-1}, B''=1.01 cm^{-1}, C''=0.88 cm^{-1}, A'=6.30 cm^{-1}, B'=1.00 cm^{-1}, C'=0.88 cm^{-1}, T_{rot}=13 K, and ν_0=10 484.2 cm^{-1}.

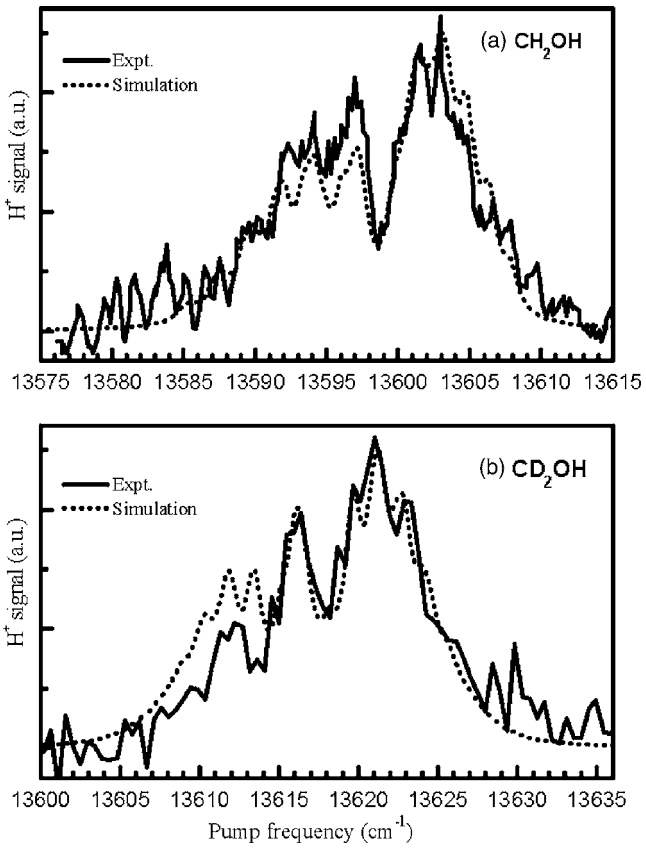

FIG. 3. The solid curve depicts experimental H-atom photofragment yield spectra in the region of the third overtone of the OH stretch for (a) CH_2OH and (b) CD_2OH. The dashed line shows a spectral fit to the data for an a-type transition and linewidth of 1.3 cm^{-1}. See text for details. In the simulations, we used $A''=6.51$ cm^{-1}, $B''=1.01$ cm^{-1}, $C''=0.88$ cm^{-1}, $A'=6.00$ cm^{-1}, $B'=B''$, $C'=C''$, $T_{rot}=13$ K, and $\nu_0=13\,597.9$ cm^{-1} for CH_2OH; and $A''=3.87$ cm^{-1}, $B''=0.86$ cm^{-1}, $C''=0.71$ cm^{-1}, $A'=3.70$, $B'=B''$, $C'=C''$, $T_{rot}=13$ K, and $\nu_0=13\,616.6$ cm^{-1} for CD_2OH.

nal. The decrease in DRID signal with time was exponential with a lifetime of 60±5 ns. The diameter of the focal spot of probe laser beam is ~0.1 mm, and that for the pump is <0.2 mm. Considering a molecular beam speed of about 1.8 mm/μs, the decay time represents mainly the fly-out time. No hydrogen fragments could be detected, consistent with the long lifetime of $3\nu_1$.

B. Excitation of the third OH-stretch overtone, $4\nu_1$

1. Hydrogen fragment yield spectra of CH_2OH and CD_2OH

Neither depletion nor DRID resulted in a clear signal above the background in the region of the $4\nu_1$ transition. This is not surprising, especially with respect to depletion, because the $4\nu_1$ transition is weaker than $3\nu_1$. As $4\nu_1$ lies well above the thermochemical threshold for dissociation to $H+CH_2O$, the next step was to monitor hydrogen fragments.

Figure 3(a) shows the $4\nu_1$ spectrum for CH_2OH obtained by monitoring hydrogen fragments by $(1+1')$ REMPI. A similar experiment was carried out with CD_2OH, in search of hydrogen and deuterium. Only hydrogen was observed and Fig. 3(b) shows the $4\nu_1$ spectrum for CD_2OH obtained by monitoring H fragments, which is blueshifted by ~19 cm^{-1} with respect to CH_2OH. The pump laser was scanned over a range of ±600 cm^{-1} around the 13 600 cm^{-1} peak of the $4\nu_1$ transition. No other transitions were detected.

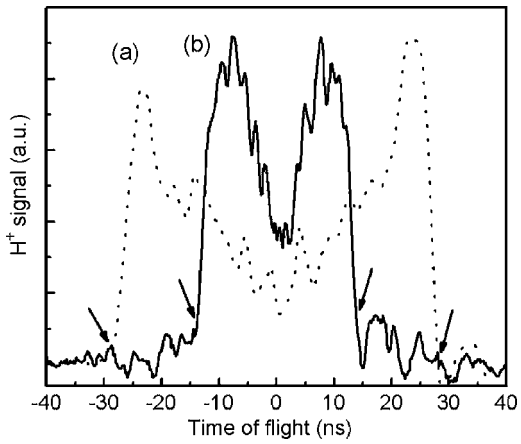

FIG. 4. Time-of-flight (TOF) spectra of H fragments produced in the dissociation of CH_2OH by one photon excitation at (a) 27 210 cm^{-1} ($3s$ Rydberg excited state) and (b) 13 603 cm^{-1} ($4\nu_1$ transition). Zero TOF indicates no recoil energy. The arrows show the maximum and minimum TOF values allowed by the thermochemistry for one-photon dissociation. The polarizations of the pump laser radiation used in (a) and (b) are perpendicular and parallel, respectively, to the extraction field. Each spectrum is a summation of 5000 laser firings, and background is subtracted.

2. Time-of-flight (TOF) analysis of hydrogen fragments

Previous studies of the transition to the lowest excited electronic state of CH_2OH, $3s$, revealed a broad and structureless spectrum with an onset at ~26 000 cm^{-1}.[12] The $3s$ state is dissociative, and near its onset H atoms are produced solely by O–H bond fission.[13] A two-photon transition via $4\nu_1$ of the ground state can access $3s$ at energies ~1200 cm^{-1} above its onset. Therefore, two possible pathways for hydrogen production via $4\nu_1$ exist: (i) one-photon unimolecular predissociation on the ground electronic state and (ii) two-photon dissociation on $3s$ mediated by $4\nu_1$ excitation.

The H-atom fragment signal varies linearly with laser fluence, which favors a one-photon process. In addition, analysis of the H-atom translational energies measured by TOF was carried out in order to determine the energetics involved in the dissociation.

Figure 4 shows TOF spectra of hydrogen fragments from CH_2OH (obtained at low repeller and extractor voltages) at two pump laser frequencies: the peak frequency of the $4\nu_1$ transition (13 603 cm^{-1}) and the doubled frequency (27 206 cm^{-1}), which can excite directly the $3s$ dissociative state. The minimum (maximum) allowed flight times corresponding to cold CH_2O cofragments flying along (opposite to) the direction of the extraction electric field are estimated by using $D_0(CH_2O-H)=9600$ cm^{-1} (Ref. 6) and are shown as the inner (outer) arrows for the two excitation energies. Clearly, the H-atom TOF distribution obtained via excitation of $4\nu_1$ is within the one-photon limit and quite different from the result obtained by doubling the frequency.

As the measured TOF spectrum is a one-dimensional projection of the velocity distribution, its main value for our purpose is in determining maximum speeds rather than the

complete velocity distributions. In particular, slower speeds are not resolved because of the convolution of angular distributions.[28] Some information on the translational energy distribution can still be obtained by lowering the extraction voltage, as seen in Fig. 4. Fast products give a better reflection of the speed distribution when the voltage is lowered, because velocity components perpendicular to the TOF axis are discriminated against. This enables us to distinguish between the energy limits associated with H fragments produced by one- and two-photon processes.

In summary, both the laser fluence dependence and the H-fragment TOF analysis support the production of fragments by one-photon dissociation. Vibrationally mediated photodissociation on $3s$ via $4\nu_1$ is unfavored. This may be due to unfavorable Franck-Condon factors for excitation from $4\nu_1$. Considering that two-photon excitation via $4\nu_1$ reaches an energy that is only 1200 cm^{-1} higher than the onset of $3s$, there is not enough energy to excite the Franck-Condon favored diagonal transitions to high OH-stretch levels. Experiments were also carried out by monitoring H-atom fragments from CD_2OH, and the results were essentially the same.

C. Spectroscopic analysis of OH-stretch overtones

CH_2OH is well described as a near-prolate asymmetric top and rotational energy levels are designated by $N_{K_aK_c}$, where N denotes the rotational angular momentum. Simulations were done with the ASYROTWIN program.[27] Ground-level rotational constants were derived from the calculated equilibrium structure,[8,26] and the upper state constants A', B', and C' were varied until a best fit to the spectra is obtained. The A rotational constants from the ground state to $4\nu_1$ (6.51,[26] 6.41 cm^{-1},[26] 6.39 cm^{-1},[26] 6.30±0.2, and 6.00±0.2 cm^{-1}, respectively) are quite similar, with a slight decrease at high overtones, reflecting probably the extension of the OH bond. However, the simulations are rather insensitive to the value of A, because the transitions are mainly a-type (parallel) bands, and higher order effects cannot be resolved.

1. Analysis of the second overtone transition

A simulated spectrum of the $3\nu_1$ transition is displayed in Fig. 2(b). The positions of the rotational transitions are shown by the stick spectrum. The transition is dominated by an a-type band with some b-type character ($I_b/I_a=0.4\pm0.2$), rather similar to the fundamental and the first overtone transitions.[26] For simplicity, only a-type transitions are assigned in Fig. 2(b). The two branches, ${}^qP$ and ${}^qR$, of the a-type transition are well resolved for the quantum number N, whereas fine rotational structures due to different K_a and K_c quantum numbers are not resolvable. For example, ${}^qR(1)$ involves three transitions with $\Delta K_a=0$, $\Delta N=1$, and $N''=1:2_{12}\leftarrow1_{11}$, $2_{11}\leftarrow1_{10}$, and $2_{02}\leftarrow1_{01}$, which can be seen in the calculated stick spectrum but are not resolved. The radical's b-type transition consists of a predominant peak of the ${}^rQ$ branch, which is overlapped with the a-type ${}^qR(2)$ transition. The rotational temperature, $T_{rot}=13\pm2$ K, is determined from the rotational level population (maximum $N''=5$ or 6) and the best-fit linewidth is 0.4±0.1 cm^{-1}—smaller than that obtained for $2\nu_1$(0.8±0.1 cm^{-1}),[26] as discussed in Sec. IV.

2. Analysis of the third overtone transition

Simulated $4\nu_1$ spectra are depicted in Fig. 3 for CH_2OH and CD_2OH. The rotational linewidths in the $4\nu_1$ transition are clearly broader than those in $3\nu_1$, with a value of 1.3 cm^{-1} for the former and 0.4 cm^{-1} for the latter. Varying the rotational temperature and the linewidth affects the spectrum differently. Specifically, for $T_{rot}=13\pm2$ K, rotational levels are populated up to $N''=5$ or 6. At higher temperatures, higher N'''s contribute more and this changes primarily the intensity distribution within the band, but has little effect on the line broadening. On the other hand, varying the linewidth changes the widths of all N''-resolved transitions, without changing their relative intensities. These two effects are quite distinct and enable us to estimate the linewidth at 1.3 cm^{-1}.

The third overtone transition can be described fairly well as an a-type band. The three branches, ${}^qP$, ${}^qQ$, and ${}^qR$, are separated from each other, whereas the transitions in each branch are overlapped and only barely separated. The line broadening of the $4\nu_1$ transition reflects the combined effect of IVR and unimolecular dissociation. Despite the higher state density of CD_2OH ($320/cm^{-1}$, compared with $110/cm^{-1}$ for CH_2OH, by the Beyer-Swinehart algorithm neglecting anharmonicity[29]), the linewidths for CD_2OH and CH_2OH are similar, suggesting that reaction rates give the dominant contribution to the linewidth (see Sec. IV).

D. Birge-Sponer analysis

Additional insight into the nature of the O–H vibrational potential can be obtained by fitting the observed vibrational levels to an expression for a Morse oscillator and comparing the extracted fundamental frequency and anharmonicity with the values for analogous OH containing molecules. The energy levels of a Morse oscillator follow the Birge-Sponer expression

$$\nu = Av - Bv^2, \tag{1}$$

where ν is the frequency of the vibration, $B=\omega_e\chi_e$ is the anharmonicity, $\omega_e=A+B$ is the harmonic frequency, and v is the number of quanta. The Birge-Sponer plots for CH_2OH shown in Fig. 5 give the (A,B) values for the ground state and the $3p_z$ excited electronic state: (3766.3±2.7 cm^{-1}, 91.4±1.0 cm^{-1}) and (3487.7±3.1 cm^{-1}, 80.5±1.4 cm^{-1}), respectively. These values are close to those for the free hydroxyl radical (3653, 82.5)[31] and other OH containing molecules, such as CH_3OH (3769.6, 86.1),[23] NH_2OH (3743, 90.6),[24] and HOOH (3701, 90.5).[24,25] The linearity of the Birge-Sponer plot is accurate for a one-dimensional (1D) Morse oscillator, and the similarity of the (A,B) parameters for all the OH containing molecules suggests that the 1D PESs along the OH coordinate are rather similar over the examined energy regions. The OH-stretch vibrational frequencies and anharmonicities derived from the Birge-Sponer expression for CH_2OH are listed in Table I.

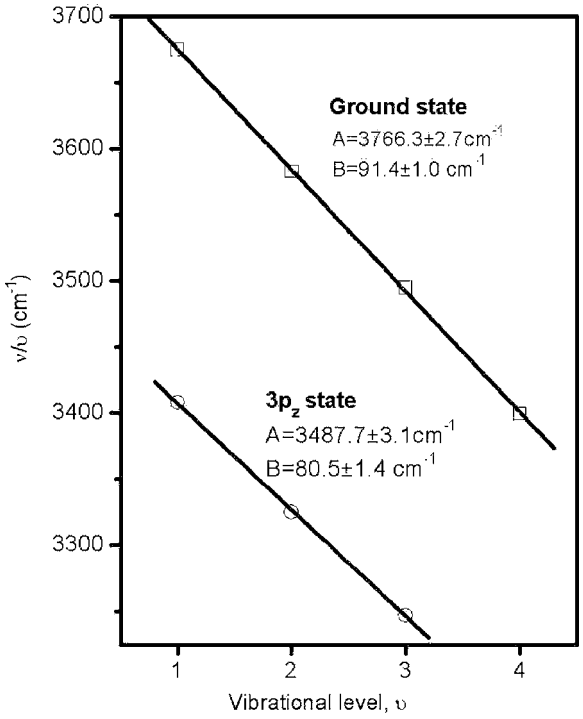

FIG. 5. Birge-Sponer plots for CH_2OH in the ground electronic state and the $3p_z$ Rydberg excited state. The experimental values for $v=1,2$ are taken from Refs. 26 and 30. The lines are fits to the Birge-Sponer expression and yield the A and B parameters indicated in the figure.

The Birge-Sponer plot of the O–H stretch overtones in the Rydberg $3p_z$ state (Fig. 5) confirms our assignment of the OH-stretch levels. Despite the fact that the $3p_z$ state is predissociative with a lifetime shorter than 0.5 ps,[12–17] the OH-stretch oscillator is less anharmonic than the ground state. A strong O–H bond is expected in $3p_z$, because the corresponding bond in the ion is stronger $[D_0(CH_2O-H^+)=59\,000\ cm^{-1}]$[8] than in the ground state of the neutral $(9600\ cm^{-1})$.[6]

IV. DISCUSSION

A. Roles of IVR, predissociation, and isomerization

The parameters characterizing the Birge-Sponer plot for the CH_2OH OH-stretch are similar to those for hydroxyl radical and other OH containing small molecules, implying that the observed transitions have a predominant local-mode OH-stretch character. In studies of overtone spectroscopy of the species containing XH stretch vibration (X=C,N,O) it has been found that the hydrogen stretch overtones are described well as local-mode vibrations.[32–38] We assume a similar local-mode behavior for the OH-stretch overtones of CH_2OH. In our previous study of $1\nu_1$ and $2\nu_1$, the $1\nu_1$ linewidth was limited by the laser bandwidth $(0.4\ cm^{-1})$, whereas the $2\nu_1$ linewidth was slightly broader $(0.8\ cm^{-1})$.[26] This broadening was explained by the existence of low-order resonances that give rise to nearby unresolved satellite bands. The linewidth of $3\nu_1(0.4\ cm^{-1})$ is narrower than that of $2\nu_1$ despite a factor of ~6 increase in the harmonic vibrational state density (from $5/cm^{-1}$ for $2\nu_1$ to $30/cm^{-1}$ for $3\nu_1$),[26,29] but is broader than the laser bandwidth in the present experiment $(0.1\ cm^{-1})$. The estimated linewidths of $4\nu_1$ for CH_2OH and CD_2OH are considerably larger $(1.3\ cm^{-1})$.

TABLE I. OH-stretch vibrational frequencies and anharmonicities of CH_2OH in the ground and the Rydberg $3p_z$ state.

	Ground	$3p_z$
ω_e/cm^{-1}	3857.7±2.9	3568.2±3.4
$\omega_e\chi_e/cm^{-1}$	91.4±1.0	80.5±1.4

The decrease in linewidth from $2\nu_1$ to $3\nu_1$ reinforces our previous conclusion that accidental low-order resonances are responsible for the observed $2\nu_1$ line broadening.[26] Because of their different anharmonicities, the levels resonant with $2\nu_1$ are detuned out of resonance with $3\nu_1$. The long lifetime of CH_2OH in $3\nu_1$ indicates that unimolecular reactions, including isomerization to CH_3O, do not contribute to the linewidth. This is not surprising, as the barriers to dissociation and isomerization are higher than the energy of $3\nu_1$ by $3000-6000\ cm^{-1}$. Measurements of linewidth as a function of laser intensity show no power broadening. The $0.4\ cm^{-1}$ linewidth of $3\nu_1$ may thus reflect homogeneous broadening due to weak couplings to bath states. In the OH overtone transitions of CH_3OH and NH_2OH, homogeneous broadening of $\sim 0.2\ cm^{-1}$ was observed starting from the second overtone of the OH stretch, which increased for higher overtones.[22,23] In OH-stretch overtones of CH_3OH, couplings due to low-order resonant states were shown to be sensitive to the value of the rotational quantum number K and the carbon isotope.[22,32]

The increased linewidth of $4\nu_1$ is likely the result of contributions from predissociation via tunneling. In order to distinguish between the contributions of IVR and lifetime broadening, the overtone spectrum of CD_2OH was also recorded. The $4\nu_1$ transition of CD_2OH is blueshifted by $19\ cm^{-1}$ from the corresponding level of CH_2OH, consistent with the OH-stretch character of the transition. Of the nine vibrational modes of hydroxymethyl, all except ν_1 (OH stretch) and ν_6 (CO stretch) are related to the motion of H(C) atoms and therefore have significantly lower vibrational frequencies in CD_2OH than in CH_2OH.[8] The different frequencies of the vibrational modes in CD_2OH and CH_2OH should result in different low-order resonances and coupling matrix elements for IVR. The observation that the two have identical $4\nu_1$ linewidths within experimental uncertainty suggests that low-order resonances are not responsible for the sharp increase in linewidth in going from $3\nu_1$ to $4\nu_1$.

Comparisons with the overtone spectroscopy of NH_2OH, HOOH, and CH_3OH are enlightening. The dissociation thresholds of these molecules are higher than that of CH_2OH and therefore lifetime broadening is insignificant in their $4\nu_1$ energy regions. The thermochemical dissociation threshold in CH_2OH is $D_0(O-H)=9600\ cm^{-1}$,[6] whereas the corresponding values for NH_2OH and HOOH are $D_0(N-O)=21\,620\ cm^{-1}$ and $D_0(O-O)=17\,052\ cm^{-1}$, respectively.[23] The OH oscillator in HOOH, for example, follows the Birge-Sponer expression up to $6\nu_1$, $2042\ cm^{-1}$ above $D_0(O-O)$, because the O–H bond energy is much higher than $D_0(O-O)$ and IVR is slow.[25] Even though $4\nu_1$ of

CH_2OH is estimated to lie ~4000 cm^{-1} above the O–H bond energy, the values of A and B returned by the Birge-Sponer plot are similar to those in the other molecules, apparently because the reaction barrier, calculated at around 15 000 cm^{-1},[6,7] traps the OH oscillator. Near the top of the barrier the energy of the vibrational levels may deviate from the Birge-Sponer straight line. For example, in HOOH, the $7\nu_1$ energy is lower by 50 cm^{-1} than the value predicted by extrapolation of the Birge-Sponer plot that describes well the lower overtones, indicating that the 1D OH potential curve is less steep at this energy than the Morse representation.[25] Our results suggest that in CH_2OH the 1D OH potential curve follows a Morse function from $1\nu_1$ to at least $4\nu_1$, with A and B values similar to those in the other OH containing molecules. This indicates that the barrier to O–H bond fission lies higher than the $4\nu_1$ level, and consequently dissociation in this energy region must proceed via tunneling.

In hydroxylamine and methanol, which have higher dissociation energies, $3\nu_1$ and $4\nu_1$ exhibit restricted IVR, and for these molecules a multitier coupling scheme, in which low-order resonances serve as gateway states to a bath of dark states, is invoked to explain the small increase in linewidth.[22,24] In contrast, in CH_2OH, which has a much lower dissociation energy, the sharp linewidth increase from $3\nu_1$ to $4\nu_1$ is most likely caused by the increased probability of unimolecular reaction.

Last, we discuss the possible contribution of isomerization to methoxy to the linewidth. In SEP studies of CH_3O, predissociation lifetimes of vibrational states of energies ~10 000 cm^{-1} were estimated to be as short as 5 ps.[9,10] No indication of decay due to isomerization to CH_2OH was obtained.[11] The heat of formation of CH_3O is higher by 2800–3200 cm^{-1} than that of CH_2OH,[4,6,8] and therefore this excitation energy is slightly lower than the energy that would have been achieved in methoxy had $4\nu_1$ excitation in CH_2OH (~13 600 cm^{-1}) led to isomerization. Such isomerization would be followed by dissociation to $H+CH_2O$, because the calculated barrier to CH_3O dissociation is lower than that for $CH_3O \leftrightarrow CH_2OH$ isomerization.[6,7] The absence of deuterium fragments following excitation of CD_2OH suggests that isomerization to CD_2HO is not favored. Also, the similarity of the $4\nu_1$ linewidths in CH_2OH and CD_2OH, which indicates similar rates for their unimolecular processes, favors direct fission of the O–H stretch.

The conclusion that isomerization is not important is reinforced by the spectroscopic studies. As mentioned above, no vibrational bands other than the OH-stretch overtone were found in the region of the $4\nu_1$ band. The geometry of the transition state for hydrogen shift from O to C has the H atom equidistant between the O and C atoms.[7] To reach this configuration, IVR to bending modes must be involved, and this should be reflected in the spectrum. The absence of such bands is another indication that isomerization does not take place and the OH stretch acts as a local mode. We conclude, therefore, that H-atom photofragments are produced by OH fission via tunneling through the barrier.

B. Predissociation by tunneling

As discussed above, the linear Birge-Sponer plot can be rationalized if we assume that the reaction barrier to direct OH bond fission is higher than the $4\nu_1$ energy. To a first approximation tunneling through the barrier can be treated by a one-dimensional semiclassical model.[39] The tunneling rate constant k is given by,

$$k = fP, \tag{2}$$

where P is the tunneling probability and f is the classical vibrational frequency given by[40]

$$f = c[\omega_e - \omega_e\chi_e(v+1)], \tag{3}$$

where c is the speed of light in vacuum. Using the ω_e and $\omega_e\chi_e$ values in Table I for the ground state, $f(4\nu_1)=1.0\times10^{14}$ s^{-1} is obtained. If we assume that the linewidth is determined exclusively by the predissociation rate ($\Gamma=1.3$ cm^{-1} or $k=2.5\times10^{11}$ s^{-1}), we obtain an upper limit to the tunneling probability, $P_{max}=2.5\times10^{-3}$.

A rough estimate of the barrier height can be obtained by using an Eckart barrier[41] with three parameters: the reaction barrier height, the dissociation energy ($D_0=9600$ cm^{-1}),[6] and the imaginary vibrational frequency ($\nu_c=1712$ cm^{-1}).[42] Assuming tunneling probabilities in the range of $P=(1.0-2.5)\times10^{-3}$, dissociation barriers of 15 100–15 400 cm^{-1} are obtained. This simple estimation compares favorably with the calculated barrier heights of 16 000 (Ref. 7) and 14 000 cm^{-1}.[6]

Evidently, lifetime broadening is not the only contributor to the $4\nu_1$ linewidth. Assuming that the homogeneous IVR broadening for $3\nu_1$ and $4\nu_1$ (0.4 cm^{-1}) are comparable, the predissociation rate should be higher than the rate of IVR. In statistical rate theories, it is assumed that IVR is rapid compared to the dissociation rate. However, for small molecules, state-specific behavior is sometimes observed as a result of incomplete IVR. The situation in CH_2OH is somewhat unique: because the reaction coordinate is excited directly, IVR is expected to hinder, rather than promote, reaction. Thus, it is plausible that reaction in the tunneling regime takes place without significant IVR.

V. CONCLUSIONS

The $3\nu_1$ and $4\nu_1$ levels of CH_2OH have been examined by overtone excitation under molecular beam conditions, and H fragments have been observed following $4\nu_1$ excitation.

The second overtone spectrum of CH_2OH was recorded by both depletion spectroscopy and DRID. The DRID spectrum is rotationally well resolved with linewidth of 0.4 cm^{-1}, reflecting IVR due to weak couplings to zeroth-order dark bath states. No dissociation is observed.

Third overtone spectra of CH_2OH and CD_2OH are obtained by monitoring H-atom fragments. They are only partially rotationally resolved, and can be simulated with similar 1.3 cm^{-1} linewidths. Both laser intensity dependence and TOF translational energy analyses support the production of H-atom fragments by one-photon dissociation from $4\nu_1$ on the ground electronic state. Considering the similar $4\nu_1$ line-

widths for CH_2OH and CD_2OH, the sharp linewidth increase from $3\nu_1$ to $4\nu_1$ is interpreted as having a major contribution from predissociation.

The linearity of the Birge-Sponer relationship indicates that the O–H overtones behave approximately as local modes of a Morse oscillator at least up to $4\nu_1$. Dissociation takes place via tunneling through the barrier to direct O–H fission. The absence of signal from D atoms, equal linewidths for CH_2OH and CD_2OH, and the absence of any other spectral features except the OH-stretch overtone indicate that IVR and isomerization to methoxy are not important. Thus, we conclude that the H-atom fission rate is faster than IVR and reaction takes place by imparting energy directly to the O–H reaction coordinate. Calculations of the potential energy surface and tunneling and predissociation dynamics will shed further light on the unimolecular processes.

An intriguing issue is what would happen when the O–H dissociation barrier is exceeded. Our attempts to excite directly the fourth OH-stretch overtone failed because the two-photon absorption cross section to the $3s$ Rydberg state exceeded the overtone excitation cross section. Sequential excitation in which $1\nu_1$ or $2\nu_1$ are first excited followed by excitation to $5\nu_1$ may be a better way to carry out these experiments.

ACKNOWLEDGMENTS

The work was supported by the Chemical Sciences, Geosciences and Biosciences Division, Office of Basic Energy Sciences, U.S. Department of Energy. The authors benefited greatly from discussions with Lin Feng, David Perry, Larry Harding, and Stephen Klippenstein and thank Larry Harding for unpublished results.

[1] J. Heicklen, *Atmospheric Chemistry* (Academic, New York, 1976).
[2] J. E. Whitten, C. E. Yong, M. J. Pellin, D. M. Gruen, and P. L. Jones, Surf. Sci. **241**, 73 (1991).
[3] K. L. Demerjian, J. A. Kerr, and J. G. Galvert, Adv. Environ Sci. Technol. **4**, 1 (1974).
[4] N. D. Petraco, W. D. Allen, and H. F. Schaefer III, J. Chem. Phys. **116**, 10229 (2002).
[5] S. Dertinger, A. Geers, J. Kappert, J. W. Wiebrecht, and F. Temps, Faraday Discuss. **102**, 31 (1995).
[6] T. P. Marcy, R. R. Diaz, D. Heard, S. R. Leone, L. B. Harding, and S. J. Klippenstein, J. Phys. Chem. A **105**, 8361 (2001).
[7] S. Saebo, L. Radom, and H. F. Schaefer III, J. Chem. Phys. **78**, 845 (1983).
[8] R. D. Johnson III and J. W. Hudgens, J. Phys. Chem. **100**, 19874 (1996).
[9] A. Geers, J. Kappert, F. Temps, and J. W. Wiebrecht, J. Chem. Phys. **101**, 3634 (1994).
[10] A. Geers, J. Kappert, F. Temps, and J. W. Wiebrecht, J. Chem. Phys. **101**, 3618 (1994).
[11] A. Geers, J. Kappert, F. Temps, and J. W. Wiebrecht, J. Chem. Phys. **99**, 2271 (1993).
[12] L. Feng, X. Huang, and H. Reisler, J. Chem. Phys. **117**, 4820 (2002).
[13] L. Feng, A. Demyanenko, and H. Reisler, J. Chem. Phys. **118**, 9623 (2003).
[14] D. Conroy, V. Aristov, L. Feng, and H. Reisler, J. Phys. Chem. **104**, 10288 (2000).
[15] B. C. Hoffman and D. R. Yarkony, J. Chem. Phys. **116**, 8300 (2002).
[16] V. Aristov, D. Conroy, and H. Reisler, Chem. Phys. Lett. **318**, 393 (2000).
[17] L. Feng, A. V. Demyanenko, and H. Reisler, J. Chem. Phys. **120**, 6524 (2004).
[18] D. R. Yarkony, J. Chem. Phys. **122**, 084316 (2005).
[19] P. J. Bruna and F. Grein, J. Phys. Chem. A **102**, 3141 (1998).
[20] P. J. Bruna and F. Grein, J. Phys. Chem. A **105**, 8599 (2001).
[21] J. A. Phillips, J. J. Orlando, G. S. Tyndall, and V. Vaida, Chem. Phys. Lett. **296**, 377 (1998).
[22] O. Boyarkin, T. R. Rizzo, and D. S. Perry, J. Chem. Phys. **110**, 11346 (1999).
[23] B. Kuhn, O. V. Boyarkin, and T. R. Rizzo, Ber. Bunsenges. Phys. Chem. **101**, 339 (1997).
[24] J. Scott, D. Luckhaus, S. Brown, and F. Crim, J. Chem. Phys. **102**, 675 (1995).
[25] B. Kuhn and T. R. Rizzo, J. Chem. Phys. **112**, 7461 (2000).
[26] L. Feng, J. Wei, and H. Reisler, J. Phys. Chem. A **108**, 7903 (2004).
[27] R. H. Judge and D. J. Clouthier, Comput. Phys. Commun. **135**, 293 (2001).
[28] Z. Xu, B. Koplitz, and C. Wittig, J. Chem. Phys. **90**, 2692 (1989).
[29] T. Bear and W. Hase, *Unimolecular Reaction Dynamics* (Oxford University Press, New York, 1996).
[30] L. Feng and H. Reisler, J. Phys. Chem. A **108**, 9847 (2004).
[31] J. Coxon and S. Foster, Can. J. Phys. **60**, 41 (1982).
[32] B. R. Henry, Acc. Chem. Res. **10**, 207 (1977).
[33] B. R. Henry and H. G. Kjaergaard, Can. J. Chem. **80**, 1635 (2002).
[34] L. Halonen, Adv. Chem. Phys. **104**, 41 (1998).
[35] I. M. Mills and A. G. Robiette, Mol. Phys. **56**, 743 (1985).
[36] M. S. Child, Acc. Chem. Res. **18**, 45 (1985).
[37] M. Quack and M. Willeke, J. Chem. Phys. **110**, 11958 (1999).
[38] A. Chirokolave, D. Perry, O. Boyarkin, M. Schmid, and T. Rizzo, J. Chem. Phys. **113**, 10068 (2000).
[39] B. Waite and W. Miller, J. Chem. Phys. **73**, 3713 (1980).
[40] G. Herzberg, *Molecular Spectra and Molecular Structure I: Spectra of Diatomic Molecules* (Van Nostrand, New York, 1950).
[41] W. Miller, J. Am. Chem. Soc. **101**, 6810 (1979).
[42] L. B. Harding (unpublished).